

Modelling and experiments of dry ice sublimation in an insulation box

A. S. Purandare^{*(a)}, S. Vanapalli^{*(a)}

^(a) Applied Thermal Sciences lab, University of Twente,
Post bus 217, 7500 AE Enschede, The Netherlands
^{*}a.s.purandare@utwente.nl; s.vanapalli@utwente.nl

ABSTRACT

A crucial aspect of the cold chain involves maintaining temperature-sensitive products at the desired temperature during transportation to guarantee the safety and quality of perishable products and fulfil regulatory requirements set by various governing bodies. Dry ice is used as a cold agent for transporting temperature-sensitive products packed inside an insulation container. Since dry ice is commercially available in multiple forms and shapes, it is essential to predict the life of various types of dry ice inside an insulation container. In this work, the sublimation process of three types of dry ice, namely, snow, pellets, and slices, placed inside an insulation container made of expanded polystyrene is experimentally and numerically investigated. It is shown that the mass of dry ice inside the insulation container, irrespective of its form, decreases linearly with time for most of the sublimation process except towards the end of sublimation.

Keywords: Cold chain, Dry ice, Sublimation, Insulation

1. INTRODUCTION

During their storage and transport, the temperature control spectrum of various temperature-sensitive goods like food, pharmaceutical, and bio-pharmaceutical products ranges from ambient (15 °C to 25 °C), refrigerated (2 °C to 8 °C), frozen (-20 °C to 0 °C), deep frozen (-80 °C to -20 °C), and cryogenic temperatures (< -150 °C). Therefore, the choice of the cold source depends on the temperature range of interest. Dry ice, a solid form of CO₂, is commonly used as a cold source for products transported under deep frozen conditions. A recent example of temperature-sensitive products transported globally on a large scale using dry ice is COVID-19 specimens and vaccines (Astori et al., 2020)(Klemeš et al., 2021).

Typically, the dry ice is packed surrounding the temperature-sensitive product in an insulated container commonly made of expanded polystyrene. The triple point pressure of carbon dioxide is above normal ambient temperature and pressure, causing only the solid and gaseous phases to exist at atmospheric conditions. As a result, the dry ice inside the insulating container constantly sublimates at -78.5 °C to form CO₂ vapor under saturated conditions. The ability of the insulation package to sustain the product's temperature at the desired level depends on the fundamental process of dry ice sublimation and heat transport mechanisms. Therefore, a thorough understanding of the dry ice sublimation and different heat transport modes (see Figure 1 for example) inside an insulation container is required to improve the efficacy of cold-chain logistics.

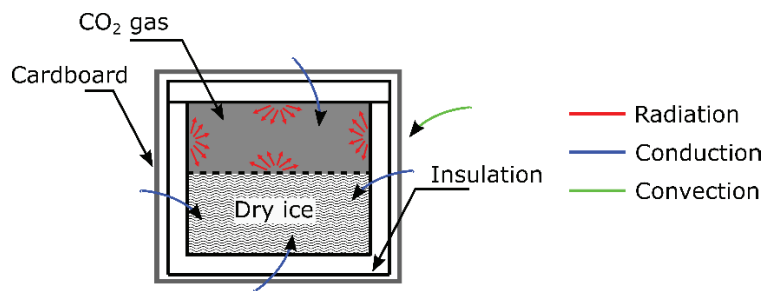


Figure 1: Schematic of different heat transfer modes for an insulation box containing dry ice

Furthermore, dry ice is commercially produced in different forms varying in density, whose impact on the lifetime of dry ice in an insulation container is not available in the open literature. Currently, the quantity of dry ice and its lifetime in the insulation container, irrespective of its type, is either predicted based on a rule of thumb or state-of-the-art models using one-dimensional heat transfer approximations. However, several uncertainties are associated with the state-of-the-art models inherent to the assumption of constant surface area between container walls and dry ice throughout the sublimation process. To overcome these limitations, a numerical model based on heat conduction and radiation was developed in our previous work to investigate the sublimation of dry ice pellets inside an insulation box (Purandare et al., 2021). The current research aims to extend the numerical model for different types of dry ice, namely, snow, pellets, and slices sublimating inside an expanded polystyrene insulation container. The model results are validated against the experimental results of the temporal evolution of the dry ice mass, sublimation rate, and temperatures inside the insulation container.

2. SUBLIMATION OF DIFFERENT FORMS OF DRY ICE

The investigation performed in this work is based on extensive comparison with experiments performed using three different types of dry ice, namely dry ice snow, pellets, and slices. Typically, high-pressure liquid CO₂ is throttled to produce dry ice with a powder-like structure. This type of dry ice is colloquially termed dry ice snow. In addition, the dry ice snow can be compressed under high pressure and die forged to form relatively high-density dry ice in cylindrical or block shapes. The former type of dry ice is called pellets, and the latter is a slice. A schematic of these dry ice types is shown in Figure 2. Typically, these forms of dry ice are packed and transported in insulation boxes along with a temperature-sensitive product of interest. During storage or transport, dry ice continuously sublimates inside the insulation box. To develop an understanding of this phenomenon, we focus primarily on the measurements of dry ice mass and temperature gradients inside the insulation box.

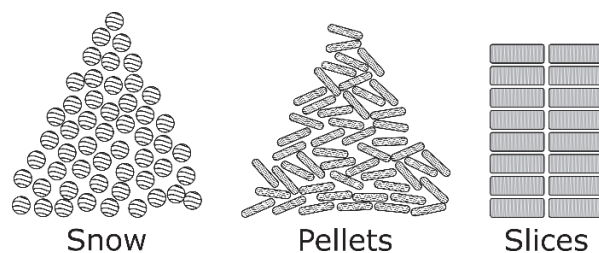


Figure 2: Schematic of different types of dry ice

2.1. Materials and Methods

Experiments were performed using a commercially available insulation box made of expanded polystyrene foam (EPS) having an external dimension of 265 x 215 x 190 mm and a wall thickness of 40 mm. The insulation box comes with a 3 mm thick fitting cardboard box. At the start of an experiment, a set of two insulation boxes is filled at the brim of the boxes with dry ice until no further dry ice can be accommodated. Then, both these boxes are placed on a weighing scale to measure the decrease in the mass of dry ice as it sublimates to form CO₂ vapor which instantaneously escapes through the thin gaps between the lid and the body of the

insulation box. One of the two boxes is equipped with several thermocouples on its inner walls at multiple locations. The experimental arrangement and a schematic of the cut section of the insulation box indicating thermocouple positions are shown in Figure 3. The mass and temperature data are recorded every three and ten seconds, respectively. The experiment is stopped when the readings of the thermocouples are close to the ambient temperature. This procedure is repeated for different types of dry ice stated in the previous section. While the dry ice snow used in the experiment is produced in-house by expanding high-pressure liquid CO₂, the pellets and slices are procured from a commercial dry ice supplier.

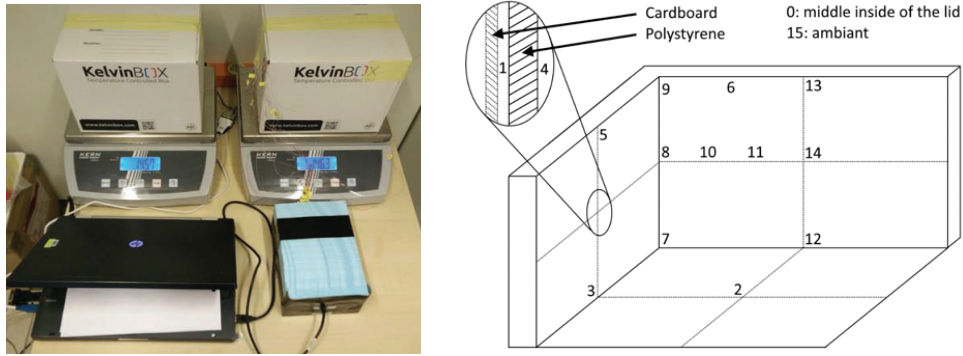


Figure 3: Experimental arrangement to measure dry ice mass and temperature inside insulation container (left); The front view cut-section of the insulation container depicting the positions of thermocouples (right)

2.2. Model

The theoretical approach taken to model dry ice sublimation inside an insulation box under quasi-static approximation is summarised in this section. The numerical model solves the three-dimensional heat conduction and radiation problem using the commercial software package COSMOL Multiphysics. The geometry defined in the model consists of four domains, namely, insulation material, cardboard box, dry ice, and CO₂ vapor as shown in Figure 4.

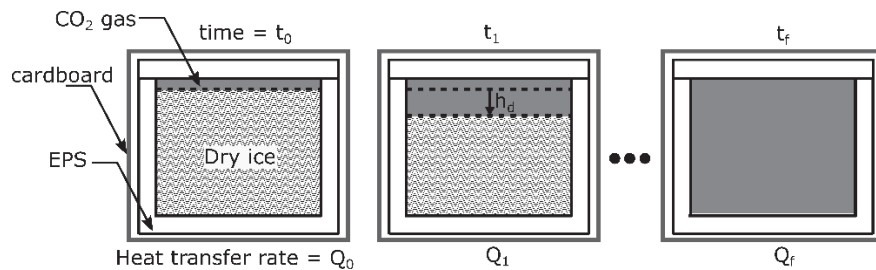


Figure 4: Schematic summarizing the approach of the numerical model. Front view cut section of the insulation container containing dry ice at different time steps is shown.

To replicate the initial situation of a filled insulation box with dry ice, a small gap of 1 mm above the dry ice interface is assumed to be occupied by the CO₂ vapor at the beginning of the simulation. At the end of this first step, the total heat transfer rate from the ambient to the dry ice via the insulation box and, in turn, the amount of dry ice mass sublimated is evaluated. In the subsequent step, the new level of the dry ice domain is calculated, assuming that the dry ice interface has uniformly shifted to its new position and is flat. At the end of every time step ($t_{i+1} - t_i$), the sublimated dry ice mass (m_i) and the corresponding decrease in the level of dry ice (h_d) is calculated from Eq. (1) and Eq. (2). Where ρ_d and l represent the packing density and the specific latent heat of dry ice, respectively. The value of the packing density is experimentally obtained, depending on the dry ice type and the inner volume, $LxWxH$ m³, of the insulation box.

$$m_i = \frac{Q_i(t_{i+1} - t_i)}{l} \quad \text{Eq. (1)}$$

$$h_d = \frac{m_i}{\rho_d LW} \quad \text{Eq. (2)}$$

This procedure is repeated until the level of the dry ice interface reaches the inner bottom surface of the insulation box, as schematically shown in Figure 4. The details of the simulation setup, including the boundary conditions used in the model, can be found in our previous work (Purandare et al., 2021).

2.3. Results and Discussion

At the start of an experiment, the packing density for each type of dry ice inside the insulation box is experimentally evaluated by dividing the initial mass of dry ice by the inner volume of the box. The percentage of the dry ice and void space inside the box is determined from the ratio of packing density and the actual density of dry ice (1565 kgm^{-3}). These parameters evaluated from one set of experimental data are presented in Table 1. While the percentage of dry ice in a given volume and, in turn, the total sublimation enthalpy is comparable for pellets and slices, they are significantly lower for dry ice snow. The data presented in Table 1 qualitatively shows differences between different forms of dry ice. The sublimation process is analysed quantitatively based on the temporal measurements of dry ice mass and temperatures inside the insulation box in the following section.

Table 1: Derived parameters for different types of dry ice when placed inside an insulation box

Dry ice type	packing density (kgm^{-3})	void space (%)	Dry ice (%)
Pellet	870	44.5	55.5
Slices	855	45.4	54.6
Snow	395	74.8	25.2

2.3.1. Variation of dry ice mass over time

The dry ice inside the insulation box will sublimate over time to form CO_2 vapor that escapes from the box to the ambient via the edges between the lid and the body of the insulation box. As a result, the mass of dry ice inside the insulation box decreases with time. The result of mass decrease measured for different types of dry ice is shown on the left of Figure 5. Since dry ice snow, pellets, and slices differ in density, the initial mass will be different to occupy a given internal volume of the insulation box. However, the density of dry ice pellets and slices is comparable; hence, the initial mass is similar. In contrast, the initial mass of dry ice snow inside a filled insulation box is significantly lower. So, naturally, the insulation box containing dry ice snow will become empty sooner than the box containing pellets and slices. However, It can be seen from Figure 5 (left) that the decrease in mass measured for all forms of dry ice is approximately linear over time for most of the sublimation process except towards the end, where deviation from the linear behavior is observed. This end effect is hypothesized to be due to the shape of the interface between dry ice and CO_2 vapor inside the box. From visual observations during the experiment, the dry ice interface becomes dome-shaped (see Figure 6) towards the end of sublimation. As a result, the contact area between dry ice and the adjacent walls reduces. This reduction in contact area decreases the heat leak into the insulation box, causing the dry ice to sublimate slower.

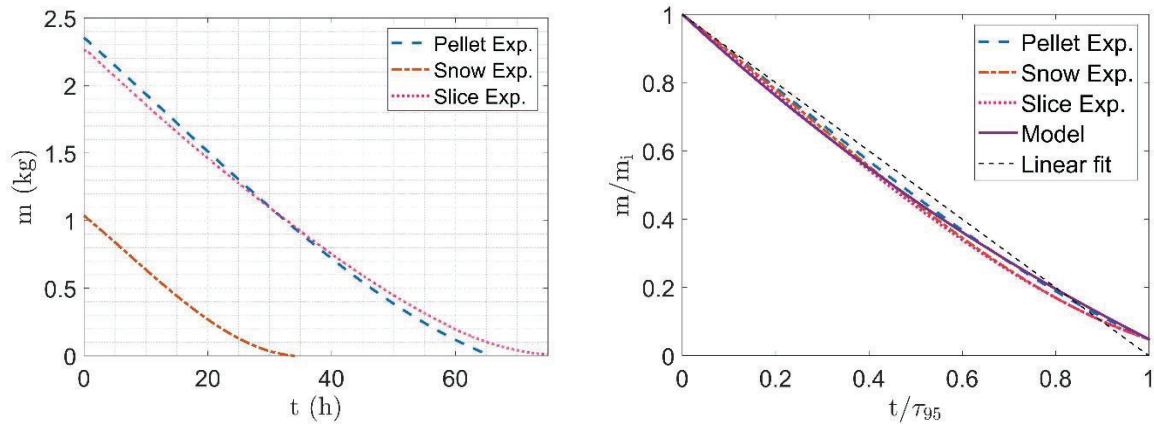


Figure 5: Temporal evolution of the dry ice mass (left: dimensional right: dimensionless) as it sublimates inside the insulation container

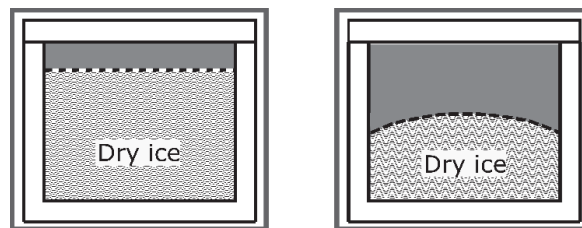


Figure 6: Schematic representation of the shape of the dry ice CO₂ vapor interface (left: assumed; right: experimentally observed)

The measured and predicted variation of the dimensionless mass of dry ice with dimensionless time for all types of dry ice is shown in Figure 5 (right). The dimensionless forms are obtained using initial mass (m_i) and time using the time taken for the dry ice to sublimate up to 95% of its initial mass (τ_{95}). The latter parameter is chosen instead of τ_{100} to neglect the end effects in this analysis. The result of the variation of the dimensionless dry ice mass with dimensionless time is shown in Figure 5 (right). It can be seen that the dimensionless mass for all forms of dry ice nearly overlaps and varies similarly with dimensionless time. From the overlap of the data, the sublimation rate of all forms of dry ice inside an insulation box would be similar if the respective ratio of the initial mass and the sublimation time, m_i/τ_{95} , is constant for all forms of dry ice. This ratio evaluated for the three types of dry ice from their respective experimental data is shown in Table 2, where the difference between the values is less than 7%. For an engineering application, this value may be considered constant, and it can be assumed that the sublimation rate of dry ice inside an insulation box for most of the sublimation process will be similar for all types of dry ice.

Table 2: Parameter, m_i/τ_{95} , evaluated for different types of dry ice

Dry ice type	m_i/τ_{95} (ghr ⁻¹)
Pellet	37.84
Snow	36.46
Slices	35.16

The numerical model is validated by comparing the predicted and measured variation of the dimensionless mass with dimensionless time, see Figure 5 (right). It is important to note that the approach used for modelling sublimation presented in this work is similar for all types of dry ice when an appropriate value of packing density, listed in Table 1, is defined for the dry ice domain. For the majority of the time, the predicted temporal evolution of the dry ice mass agrees reasonably well with the measured data. A reference fitting line intercepting at (1,0) on the x-axis and (0,1) on the y-axis, respectively, is plotted in Figure 5 (right) to graphically show that the temporal evolution of the mass of dry ice, irrespective of its form, is approximately

linear for the majority of the time. A noticeable deviation between the model and experimental results at later times can be ascribed to two main reasons. First, the shape of the dry ice-CO₂ vapor interface inside the box is assumed to be flat, but in reality, the shape will deform over time, influencing the heat leak and the sublimation rate of dry ice. Secondly, the material properties of EPS are assumed constant. In practice, the temperature of the insulation box changes over time, which in turn influences an important thermal property of EPS, namely, its thermal conductivity. In this work, the thermal conductivity of EPS is evaluated at the mean temperature of dry ice and ambient (20 °C), i.e. at -30 °C, from the empirical relationship provided in the work of Gnip et al. (2012). Despite the simplifications, the numerical model can predict the behavior of dry ice sublimation inside the insulation box reasonably well up to engineering accuracy.

2.3.2. Variation of insulation temperature over time

The temperature data measured at different locations inside the insulation box containing dry ice pellets and slices are shown in Figure 6. In both cases, the temperature at the bottom center (T2) is approximately constant throughout the sublimation process, whose value is close to the sublimation temperature of dry ice. This is because dry ice is in the vicinity of the thermocouple on the bottom face of the insulation box until the end of the sublimation process. The wiggles seen in the temperature data measured by thermocouples T3, T7, and T12 in the case of the insulation box containing pellets are presumably due to the intermittent contact by the pellets. This behavior is observed only in the case of pellets because, given the shape of pellets, they can slide and move towards the edges to make contact with the thermocouples during sublimation. The temperature of the inner vertical walls of the insulation box, measured by all thermocouples except T2 and T15, containing dry ice slices is marginally higher than that of the box containing pellets. This may be attributed to the ample void space due to the less uniform distribution of slices inside the insulation box used during experiments. Since the heat leak is proportional to the temperature difference between the insulation box's ambient and inner walls, dry ice slices inside the insulation box take marginally longer to sublimate than the pellets, as seen in Figure 5 (left).

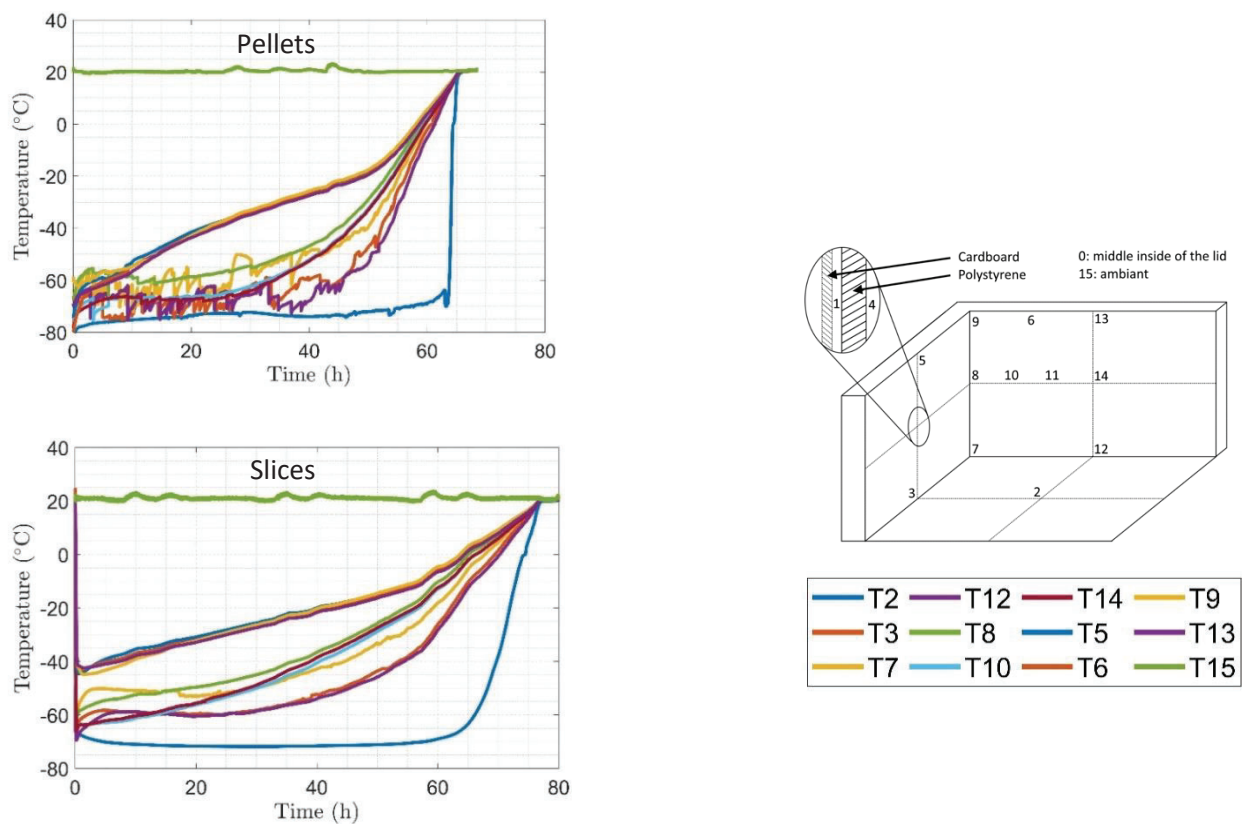


Figure 7: Measured temperature variation inside insulation box containing dry ice pellets (top left) and slices (bottom left). Schematic of the front view cut section of the insulation box representing thermocouple positions.

To summarize, dry ice snow occupies larger volumes per unit mass than pellets and slices. Therefore, the lifetime of dry ice snow inside an insulation box is lower than that of pellets and slices occupying the same box volume. However, the measured temporal characteristics of the dry ice mass and temperatures inside the insulation container are similar for all types of dry ice, which agree reasonably well with model predictions for most of the sublimation process. From a future perspective, it is imperative to model and experimentally investigate the transient deformation of the dry ice interface and incorporate relevant flow dynamics in the CO₂ vapor domain to understand further the fundamental phenomenon of dry ice sublimation inside the insulation box.

3. CONCLUSIONS

In this paper, sublimation inside an insulation container for different types of dry ice is investigated experimentally and numerically. The numerical model developed in our previous work to examine the sublimation of dry ice pellets in an insulation box is successfully extended to model the sublimation of dry ice snow and slices. A vital parameter input to the model that changes with the dry ice type is its packing density, which is experimentally determined from the insulation container's initial mass and internal volume. The predicted results from the model are validated against the measured values of the temporal evolution of dry ice mass and temperatures inside the insulation box. Unlike the state-of-the-art models, the numerical model presented in this work accurately predicts the heat leak and the quantity of a given dry ice inside an insulation box which could be helpful for several shippers in transporting/storing a temperature-sensitive product.

ACKNOWLEDGEMENTS

This work is supported by the funding received from Air Liquide. In addition, we would like to thank Jean-Pierre Bernard, Senior Project Manager Air Liquide, for numerous discussions and valuable input during the execution of this project.

NOMENCLATURE

L, W, H	Length, width, and height of inner side of insulation container (m)	h_d	Decrease in level of dry ice (m)
t	Time (s)	m	Sublimated dry ice mass (kg)
Q	Heat transfer rate from the ambient into the insulation container (W)	l	Specific latent heat of sublimation of dry ice (571 kJkg ⁻¹)
τ_{95}	Time taken for the dry ice to sublimate up to 95% of its initial mass (s)	ρ_d	Packing density of dry ice inside insulation container (kgm ⁻³)
m_i	Initial mass of dry ice inside insulation container (kg)		

REFERENCES

- Astori, G., Bernardi, M., Bozza, A., Daniela, C., Katia, C., Merlo, A., Santimaria, M., Barbazza, R., Amodeo, G., Ciccocioppo, R., Elice, F., Ruggeri, M., 2020. Logistics of an advanced therapy medicinal product during COVID-19 pandemic in Italy: successful delivery of mesenchymal stromal cells in dry ice. *J Transl. Med.* 18.
- Gnip, I., Vejelic, S., Vatikus, S., 2012. Thermal conductivity of expanded polystyrene (eps) at 10 °C and its conversion to temperatures within interval from 0 to 50 °C. *Energy and Buildings.* 52.
- Klemeš, J. J., Jiang, P., Fan, Y., Bokhari, A., Wang, X., 2021. COVID-19 pandemics Stage II – Energy and environmental impacts of vaccination. *Renewable and Sustainable Energy Reviews.* 150.
- Purandare, A.S., van Lohuizen, S.W., Spijkers, R.M.A., Vanapalli, S., 2021. Experimental and numerical study of insulation packages containing dry ice pellets. *Applied Thermal Engineering.* 186.